Supporting Information for:

Aggregation-induced emission and polymorphism/shape/size-dependent emission behaviours of fenamates for potential drug evaluation

Xinyi Wang,[ab†] Yifu Chen,[ab†] Junbo Gong,[*ab] and Jinze Hou[ab]

[a.] State Key Laboratory of Chemical Engineering, School of Chemical Engineering and Technology, Tianjin University, Weijin Road 92, Tianjin, 300072, P.R. China.

[b.] Collaborative Innovation Center of Chemistry Science and Engineering, Weijin Road 92, Tianjin, P.R. China.

[†] X.W. and Y.C. contributed equally to this work as first authors.

Org. Biomol. Chem.

List of Contents

Powder X-ray Diffraction Patterns

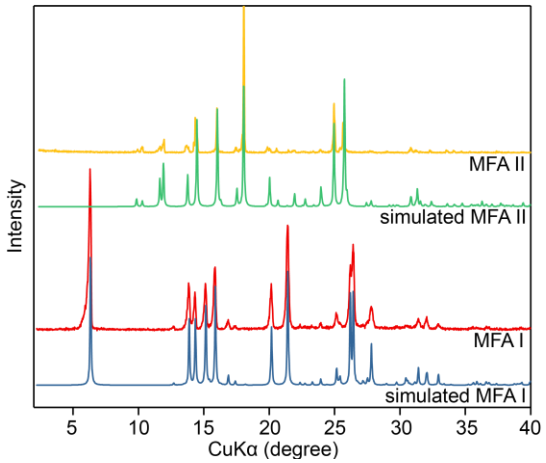

Figure S1. Simulated crystallographic diffraction patterns of *MFA I* and *MFA II* (simulated from available single-crystal structure from the Cambridge structural database, CCDC 1298182 and CCDC 1441832) and X-ray powder diffraction patterns of the prepared *MFA I* and *MFA II*, respectively.

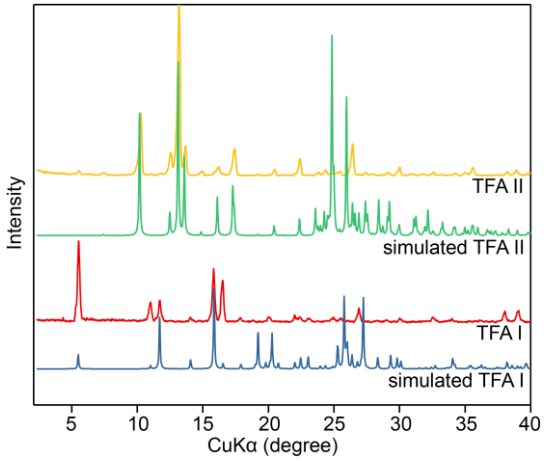

Figure S2. Simulated crystallographic diffraction patterns of *TFA I* and *TFA II* (simulated from available single-crystal structure from the Cambridge structural database, CCDC 1193604 and CCDC 1193603) and X-ray powder diffraction patterns of the prepared *TFA I* and *TFA II*, respectively.

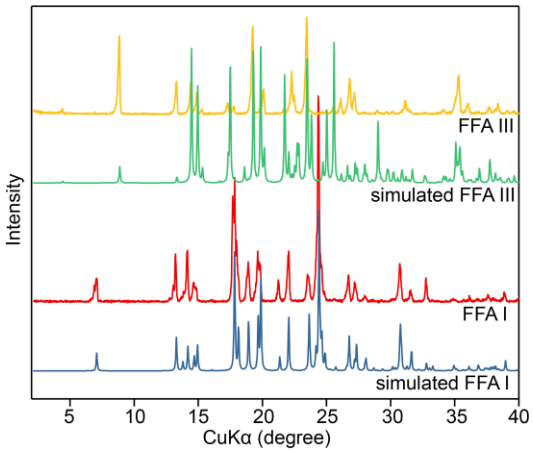

Figure S3. Simulated crystallographic diffraction patterns of *FFA I* and *FFA III* (simulated from available single-crystal structure from the Cambridge structural database, CCDC 1160200 and CCDC 1160195) and X-ray powder diffraction patterns of the prepared *FFA I* and *FFA III*, respectively.

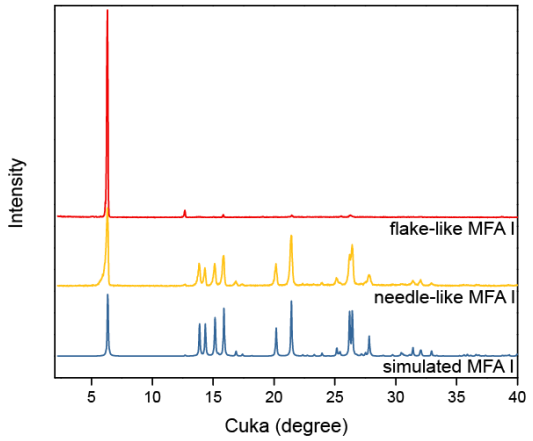

Figure S4. Simulated crystallographic diffraction patterns of *MFA I* (simulated from available single-crystal structure from the Cambridge structural database, CCDC 1298182) and X-ray powder diffraction patterns of the prepared *MFA I* with different shapes.

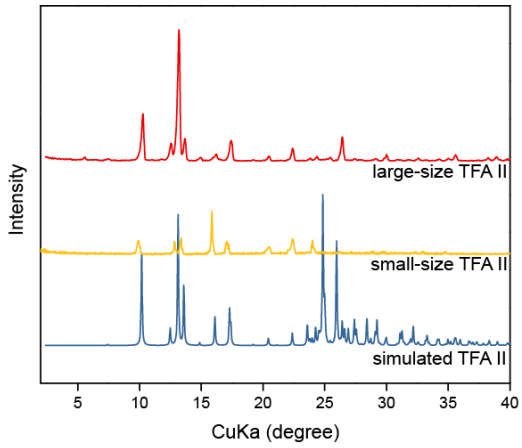

Figure S5. Simulated crystallographic diffraction patterns of *TFA II* (simulated from available single-crystal structure from the Cambridge structural database, CCDC 1193603) and X-ray powder diffraction patterns of the prepared *TFA II* with different sizes.

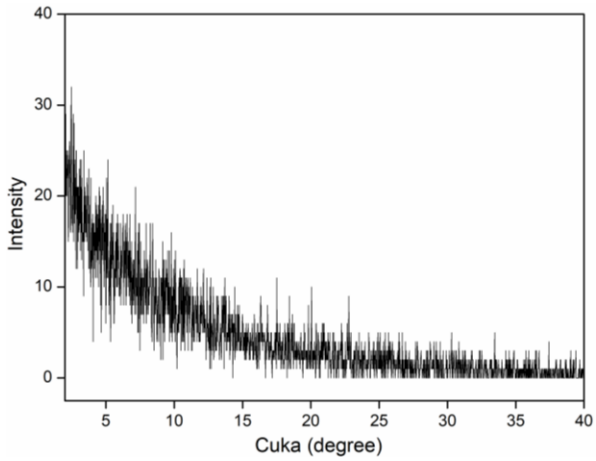

Figure S6. The X-ray powder diffraction pattern of amorphous form of *MFA.*

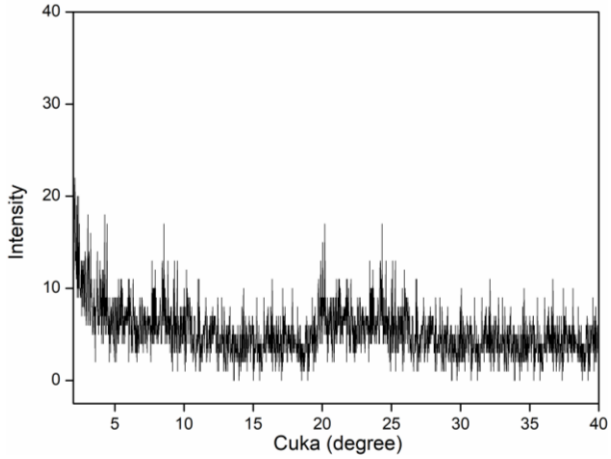

Figure S7. The X-ray powder diffraction pattern of amorphous form of *TFA.*

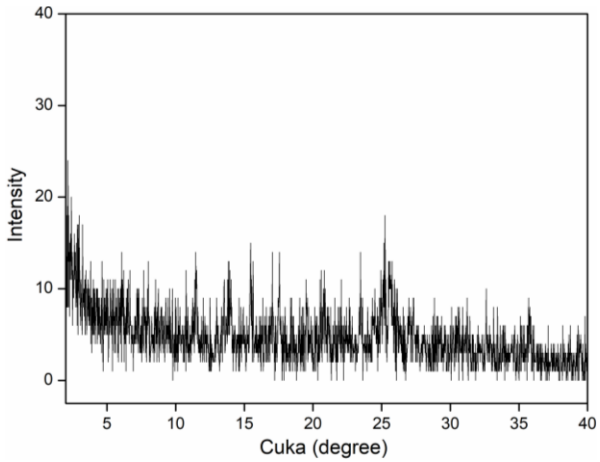

Figure S8. The X-ray powder diffraction pattern of amorphous form of *FFA.*

Fluorescence Characterizations and Absorption Spectra

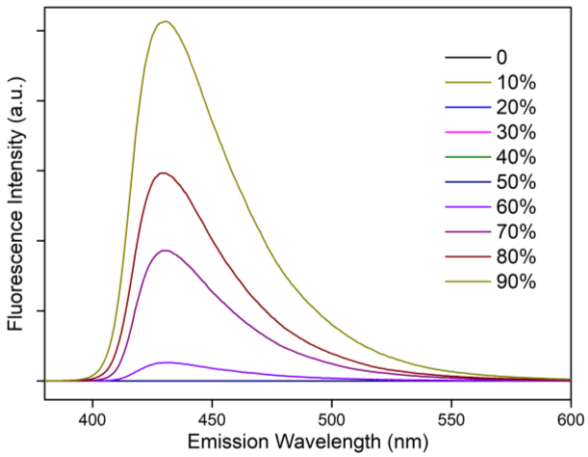

Figure S9. PL spectra of solution of *MFA I* in the ethanol−water solvent system with different water fractions under 365 nm UV illumination.

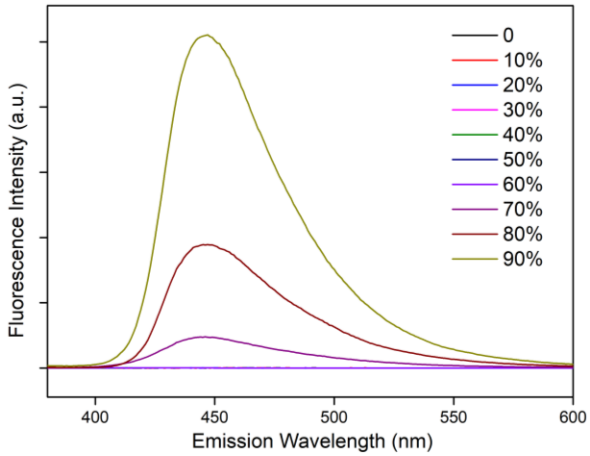

Figure S10. PL spectra of solution of *FFA I* in the ethanol−water solvent system with different water fractions under 365 nm UV illumination.

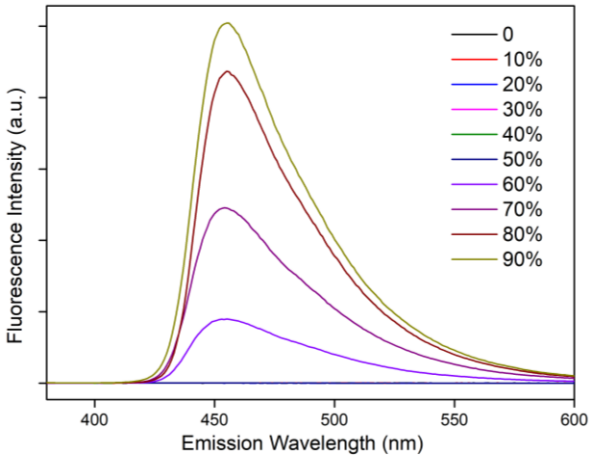

Figure S11. PL spectra of solution of *FFA III* in the ethanol−water solvent system with different water fractions under 365 nm UV illumination.

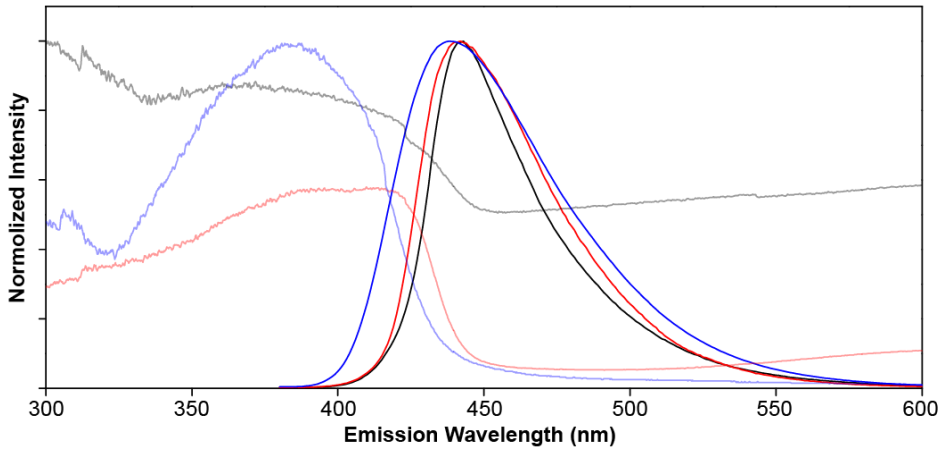

Figure S12. PL spectra of *MFA I* (bright black color), *MFA II* (bright red color) and amorphous form of *MFA* (bright blue color) under a fixed excitation wavelength of 365 nm. UV-Vis diffuse reflectance spectra of *MFA I* (light black color), *MFA II* (light red color) and amorphous form of *MFA* (bright blue color).

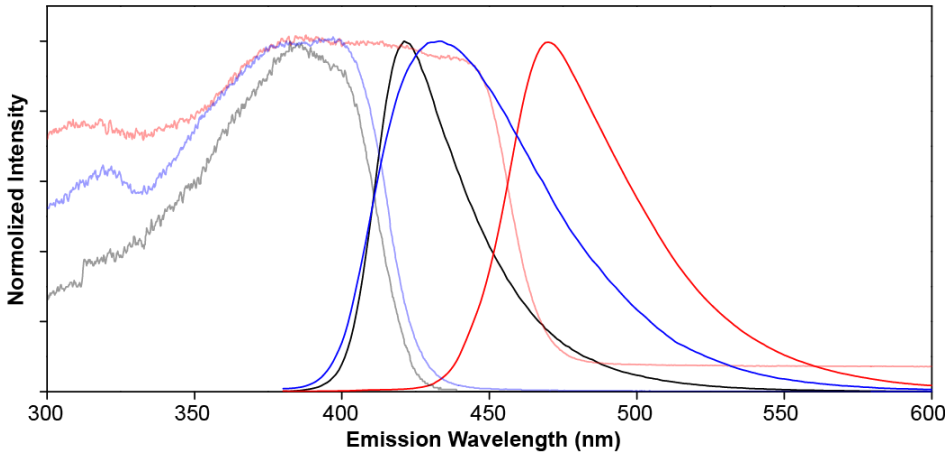

Figure S13. PL spectra of *TFA I* (bright black color), *TFA II* (bright red color) and amorphous form of *TFA* (bright blue color) under a fixed excitation wavelength of 365 nm. UV-Vis diffuse reflectance spectra of *TFA I* (light black color), *TFA II* (light red color) and amorphous form of *TFA* (bright blue color).

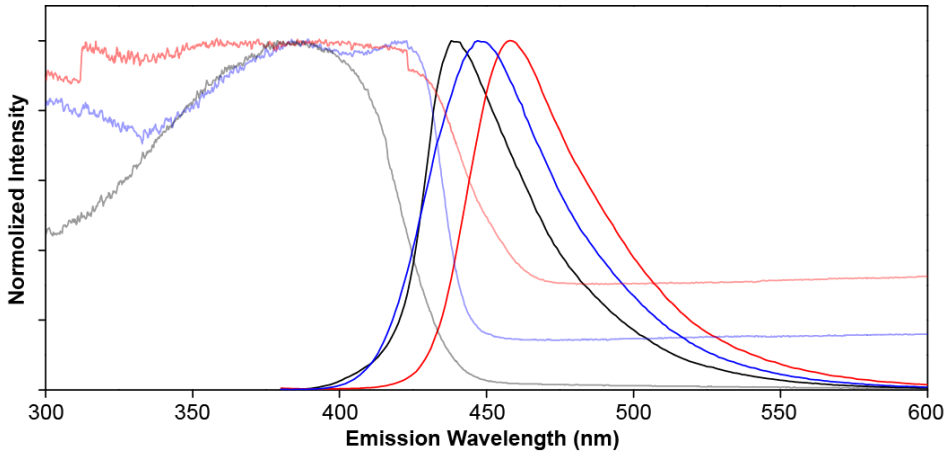

Figure S14. PL spectra of *FFA I* (bright black color), *FFA III* (bright red color) and amorphous form of *FFA* (bright blue color) under a fixed excitation wavelength of 365 nm. UV-Vis diffuse reflectance spectra of *FFA I* (light black color), *FFA III* (light red color) and amorphous form of *FFA* (bright blue color).

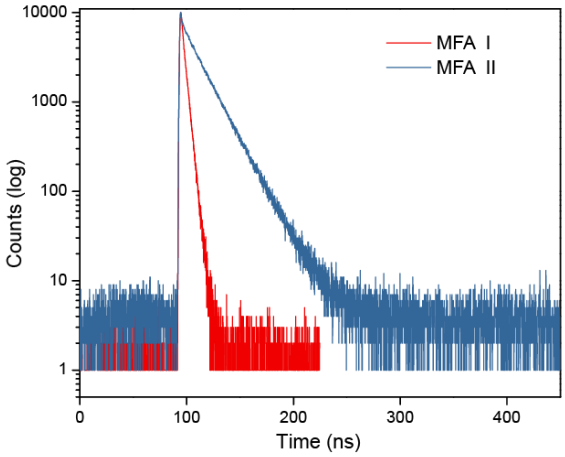

Figure S15. Nanosecond time-resolved photoluminescent dynamic of the *MFA I* and *MFA II*.

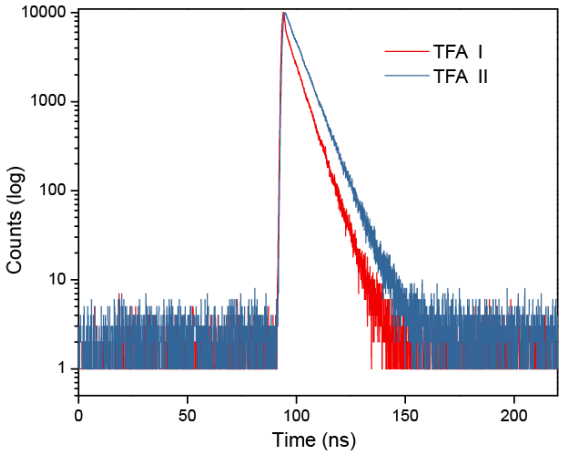

Figure S16. Nanosecond time-resolved photoluminescent dynamic of *TFA I* and *TFA II*.

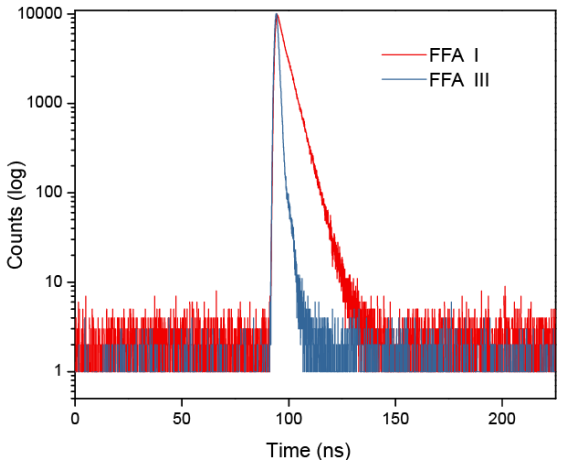

Figure S17. Nanosecond time-resolved photoluminescent dynamic of *FFA I* and *FFA III*.

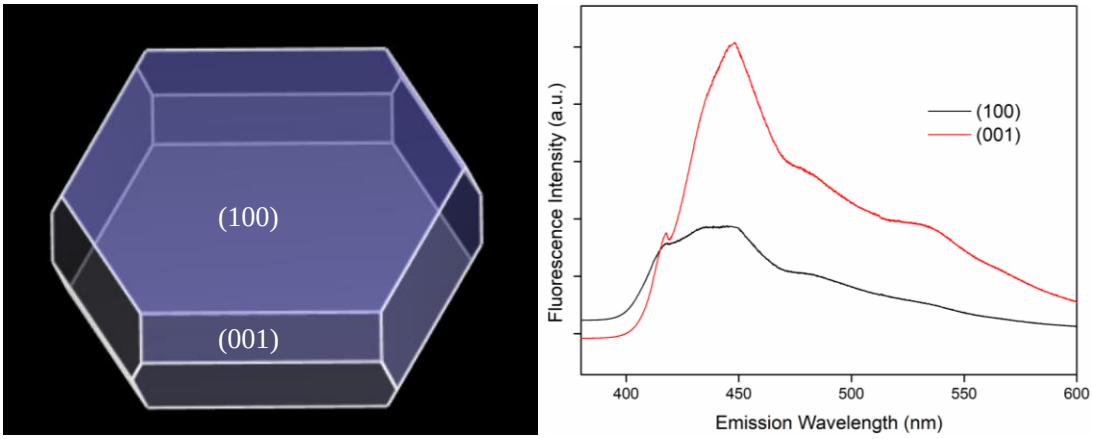

Figure S18. The predicted growth morphology of *MFA I* in vacuum and fluorescence emission spectra of *MFA I* with different crystal faces.

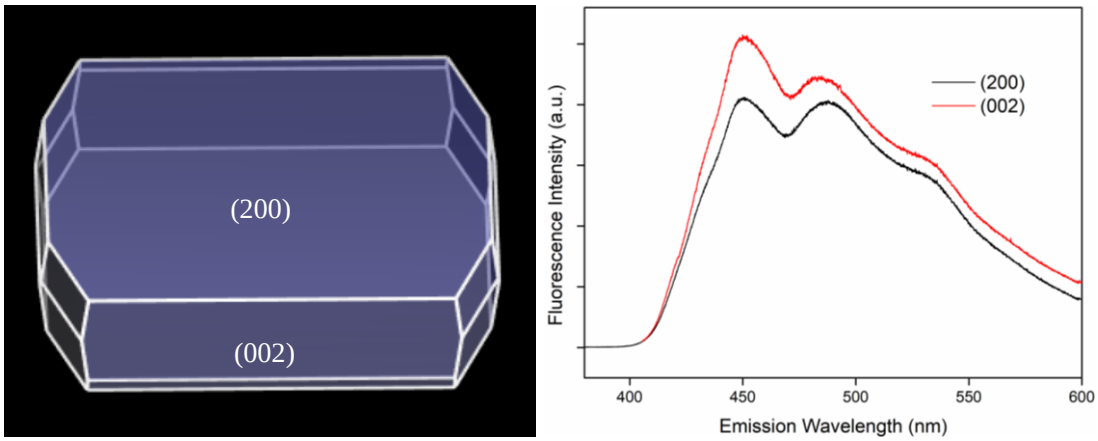

Figure S19. The predicted growth morphology of *FFA III* in vacuum and fluorescence emission spectra of *FFA III* with different crystal faces.

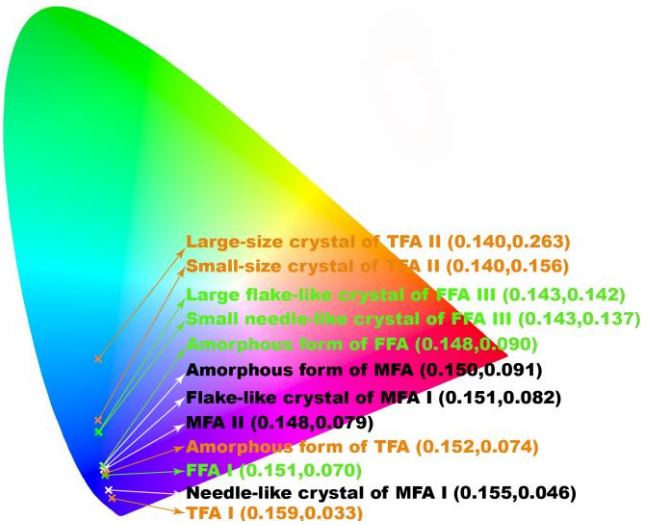

Figure S20. CIE 1931 chromaticity diagram. The cross indicates the CIE coordinates for different solid states of fenamates.

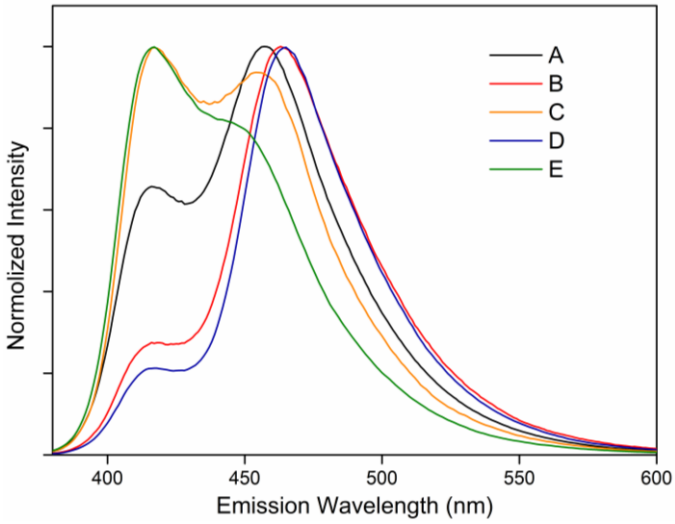

Figure S21. PL spectra of polymorphs quantitative analysis for TFA.

Additional Photos and Microphotographs

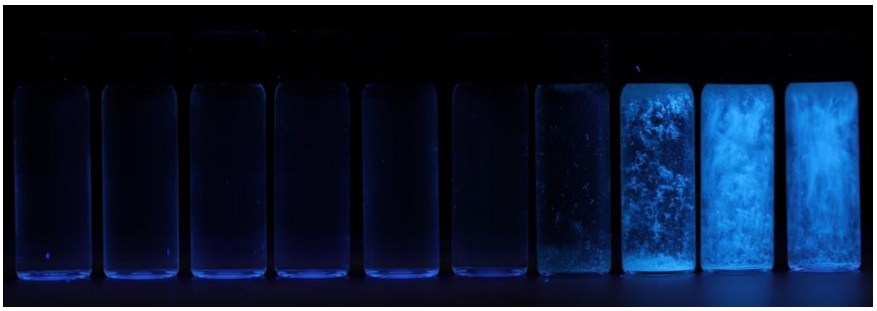

Figure S22 Fluorescent image of *MFA I* in the ethanol−water solvent system with different volumetric ratio of water (0-90 %) under 365 nm UV illumination.

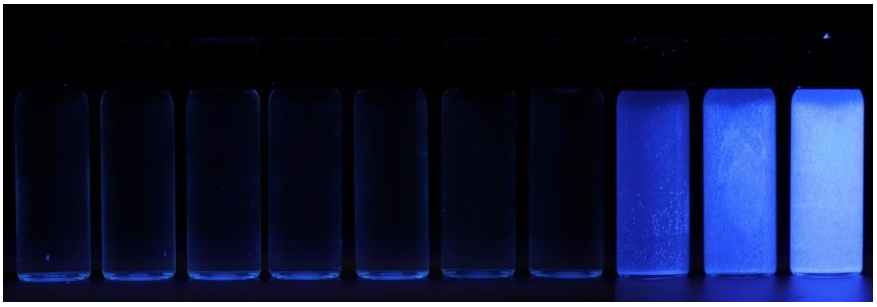

Figure S23 Fluorescent image of *FFA I* in the ethanol−water solvent system with different volumetric ratio of water (0-90 %) under 365 nm UV illumination.

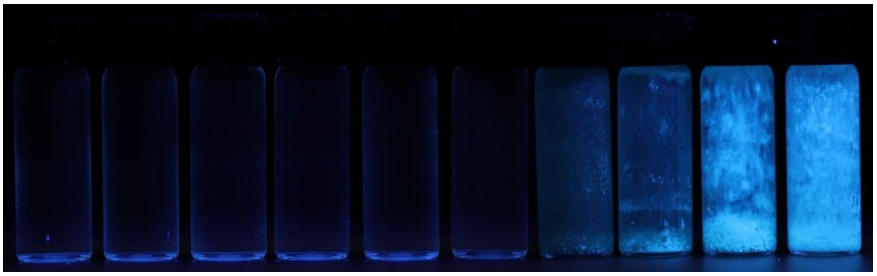

Figure S24 Fluorescent image of *FFA III* in the ethanol−water solvent system with different volumetric ratio of water (0-90 %) under 365 nm UV illumination.

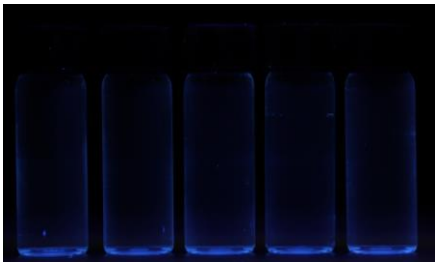

Figure S25 Fluorescent image of *TFA II* in the ethanol−water solvent system with different volumetric ratio of water (0-40 %) under 365 nm UV illumination.

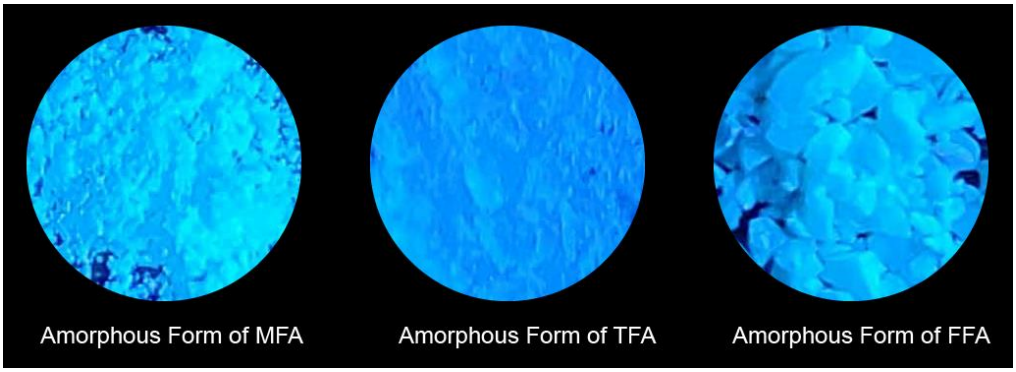

Figure S26 Fluorescent image of amorphous form of *MFA*, *TFA* and *FFA* under 365 nm UV illumination.

The Supplementary Table

Table S1 The verification experiment of polymorphs quantitative analysis.

Sample	A	B	C	D	E
TFA I (mg)	22.8	34.0	17.2	38.0	13.6
TFA II (mg)	17.2	6.0	22.8	2.0	26.4
Actual mass ratio of TFA I	57.0	85.0	43.0	95.0	34.0
Calculated mass ratio of TFA I	59.4%	83.0%	45.3%	97.2%	35.8%